Thermal analysis of metal organic precursors for functional oxide preparation: thin films versus powders

P. Roura[1*], J. Farjas[1], H. Eloussifi[1], L. Carreras[1] , S. Ricart[2], T. Puig[2], X. Obradors[2]

1) GRMT, Dept. of Physics, University of Girona, Campus Montilivi, Edif. PII, E17071 Girona, Catalonia, Spain

2) Institut de Ciència de Materials de Barcelona, Consejo Superior de Investigaciones Científicas (ICMAB-CSIC), Campus de la UAB, 08193 Bellaterra, Catalonia, Spain

* Corresponding author: pere.roura@udg.cat, FAX (34) 972418098

Abstract

The thermal decomposition of several metal organic precursors, used in the preparation of $YBa_2Cu_3O_{7-x}$ superconducting coated conductors (Cu acetate, Cu, Y and Ba trifluoroacetates and Ce propionate), is analyzed by means of several thermoanalytical techniques (TG/DTA, MS and DSC). In all cases, the metal organic precursors deposited as films decompose differently than powders of the same precursors. In films, decomposition is facilitated by the easier transport of reactive gas from the surrounding atmosphere and by the easier out-diffusion of volatile products. It is also shown that the good thermal contact with the substrate minimizes overheating and avoids combustion. Finally, the formation and stability of intermediate products towards the oxide formation, such as metal fluorides, is different in films because of the easier gas exchange. Although, in some cases, the behaviour of films can be predicted by analyzing varying masses of precursor powders, this is not always the case. Therefore, thermal analysis carried out on films is recommended to avoid erroneous conclusions about materials preparation drawn from powders.

Keywords: pyrolysis, thermal decomposition, YBCO, TGA, DTA, EGA

I.- Introduction

Thermal decomposition of metal organic precursors is a current route for the synthesis of metal oxides in the form of powders, thin films or nanostructures [1,2,3,4,5,6]. Films can be obtained by Chemical Solution Deposition (CSD) techniques. A solution containing the precursor is spread over a substrate and, after solvent evaporation, the film is pyrolyzed. By controlling the precursor concentration and spreading conditions, film thickness can vary from tens of nm to several microns. These techniques allow fabrication of low-cost oxide single or multilayers that find application in microelectronics [7], high-temperature superconductors [8, 9, 10], photovoltaic energy conversion [11], optical layers [12], ferroelectric devices [13], etc.

The oxide quality critically depends on the pyrolysis conditions (heating rate to the isothermal stage, temperature and furnace atmosphere) when metal organic decomposition takes place. At this point, thermoanalytical techniques (notably thermogravimetry (TG) coupled with mass spectrometry (MS) or infrared spectroscopy) are very useful because they give information about the decomposition temperature, decomposition mechanism and kinetics and allow prediction of the evolution of the reaction when the material is submitted to a particular temperature program [14]. Since the signal delivered by any technique is proportional to the sample mass, m_i, thermal analysis experiments are usually done with the precursor in the form of powders (typically, $m_i > 5$ mg)[7, 15], whereas experiments on films are very scarce (typically, $m_i < 1$ mg/cm^2)[16]. This is so because, for the low masses of films, the TG baseline instability impedes the accurate analysis of the decomposition mass-loss curve. Consequently, the question arises: “Is the information delivered by powders (e.g. decomposition temperature, final or intermediate products and their dependence on the atmosphere) valid for films?”

In this paper, we will show that, in general, owing to the large difference in surface-to-volume ratio between films and powders, the restricted gas transport between particle interstices in powders and the better thermal contact with the substrate in films one should expect a negative answer whenever the decomposition kinetics is controlled by a transport step. To be more specific, films are expected to decompose differently than powders when the decomposition is controlled by: a) transport of reactive gas (usually O_2 or H_2O); b) evolution of gaseous species (reaction products or solvents) or c) heat transport out of the sample (see the summary given in Fig.1). All these aspects are not exclusive of decomposition processes but are intrinsic to most solid-gas reactions [10]. The fact is that, for most

precursors we have analyzed to date, significant differences have been observed between powders and films. So, it is clear that optimization of the pyrolysis step can be hardly achieved with thermal analyses on powders. It is necessary to develop experimental procedures for measuring the decomposition directly on films or, alternatively, to establish criteria that would help to deduce the behaviour of films from that of powders.

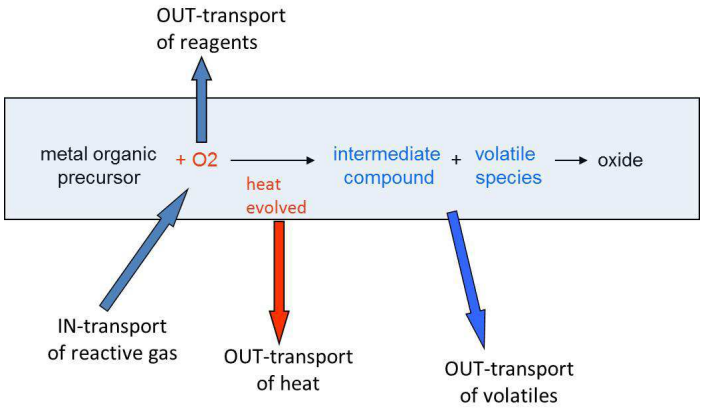

Figure 1.- Scheme showing several transport processes that can have some influence on the formation and microstructural development of oxide powders and films.

Substrates can also have a catalytic effect on decomposition reactions through its chemical terminations *(e.g. H^+ terminations on the surface of glass substrates enhance decomposition of $Y(TFA)_3$ [18])* or by promoting epitaxial growth of the oxide. *Film deposition requires preparation of a solution that may modify the precursor molecular structure. These effects are not related to any transport mechanism and will be not analysed here.*

The examples given below correspond to metal organic precursors used for the fabrication of $YBa_2Cu_3O_{7-x}$ (YBCO) superconducting tapes. These tapes consist in the active superconductor layer (1-2 μm thick) separated from the metallic substrate by one or several oxide thin buffer layers such as ceria (CeO_2) or other oxides [4, 19].

II.- Experimental section

Most precursors were used in their commercial form of powders except Ce propionate that was synthesised from Ce acetate (see details in [20]). The powders were analysed inside alumina pans without cover to facilitate gases exchange. To obtain thin films, the precursor salts were dissolved in acetic or propionic acid and, then, a microdrop was spread on an appropriate substrate and dried below 100ºC or, alternatively, a spin coater was used. Thin glass discs, platinum foils or silicon and

(001)$LaAlO_3$ single crystalline substrates were used depending on the experiment. To increase the mass of the samples, films were deposited on both substrate sides and several (usually two) substrates were kept some mm apart inside the TG furnace, to allow gas exchange with the furnace atmosphere. *The as-deposited films were dense and not simple aggregates of powders as revealed by optical microscopy*. The thickness of the films is their "nominal thickness", i.e. the thickness the film would have if transformed into a dense oxide.

TG analyses were done with a TGA851^{e}LF apparatus from Mettler Toledo and a Setsys Evolution apparatus from Setaram under continuous flow of high-purity gases (usually 40 mL/min). The TG curves were corrected by the apparatus baseline, measured during a consecutive measurement under identical conditions. Additionally, the final mass of the sample was always measured and compared with that deduced from the TG curve. Significant discrepancies led us to discard experiments. These precautions were essential for the experiments on films. These apparatus simultaneously delivered the differential thermal analysis signal (DTA). For the differential scanning calorimetry (DSC) measurements, the DSC822 from Mettler Toledo was used. And, finally, mass spectroscopy (MS) measurements were taken simultaneously to the TG curves with an MKS Spectra Quadrupole (Micro Vision Plus), which detects molecular fragments with m/z < 300 amu.

Several apparatus were used for the X-ray diffraction experiments (XRD): a) Smart Apex diffractometer of Bruker AXS (with Mo x-ray source) where collection of the diffracted photons was done with a CCD detector that increases the experimental sensitivity at the expense of resolution; b) conventional D8 Advance diffractometer from Bruker AXS in the $\theta - 2\theta$ configuration (Cu x-ray source); and c) thin film diffractometer PANalytical model X'pert PRO MRD (Cu x-ray source). XRD spectra were analyzed using eva software from SOCABIM and the JCPDS database from the International Centre of Diffraction Data.

III.- Results and discussion

III.1.- Transport of reactive gas: decomposition of Ce propionate

When the decomposition temperature, T_{dec}, is higher in inert atmosphere than in reactive atmosphere this means that the reactive gas plays a role in the decomposition. Consequently, when its transport is easier, decomposition should occur before. This leads us to predict a diminution of T_{dec} in reactive atmosphere for smaller sample masses, m_i. Consequently, films should decompose at a lower temperature than powders.

The dependence on m_i is easily understood as due to the reactive gas consumption at the sample surface. Higher m_i implies faster gas consumption and, consequently, a less reactive atmosphere near the sample (this effect has also been observed during nitruration of Si micro and nanoparticles [17]). Thus, T_{dec} must approach the value for inert conditions when m_i increases. For films, the high surface to volume ratio facilitates gas transport of reactive gas from the furnace to the sample surface and its diffusion through the material and, consequently, T_{dec} will be minimal for thin films.

These predictions are nicely illustrated by the TG curves corresponding to the decomposition of Ce propionate in air and in N_2 (Fig. 2). Notice that T_{dec} in air diminishes with m_i and that the decomposition begins at the same temperature than in inert atmosphere when m_i is high enough (above 10 mg). The thinnest film we have measured (m_i = 0.25 mg/cm^2) decomposes at around 120ºC below the decomposition temperature of 10 mg of powders. This difference gives us an idea of the great errors that can be done if one applies to the films the information obtained from powders.

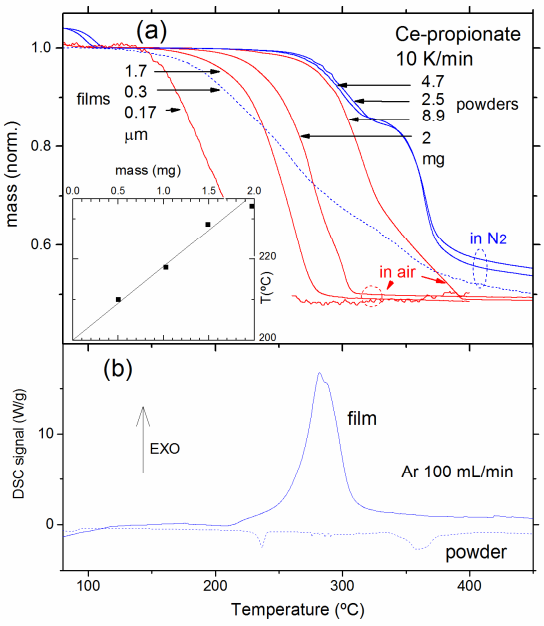

Figure 2.- a) TG decomposition curves of Ce propionate films and powders in air (solid lines) and in N2 (dashed lines). Quoted film thicknesses refer to the expected thickness of dense CeO2 films. Inset: dependence of the decomposition temperature (mass = 0.9) on the initial mass of powders. b) DSC curves measured in a nominally inert atmosphere.

In principle, one would expect that, at the limit m_i --> 0 both powders and films should decompose at the same temperature. From the inset of Fig. 2, T_{dec} in air is predicted to be 200 ºC at this limit, whereas the thinnest film decomposes at 170 ºC. This discrepancy can be due either to the fact that gas exchange

between the sample and the furnace is more difficult when the sample is located inside a crucible (even without cover) or to the longer diffusion distance inside powder particles.

For experiments done in inert atmosphere, T_{dec} should be independent of m_i and share the same value for films and powders. In Fig. 2 we see that the curves coincide for powders above 2.5 mg. However, and surprisingly, a thin film begins to decompose at a much lower temperature. We consider that, in this case, the residual oxygen partial pressure in the furnace was high enough to enhance the decomposition rate of the film whereas it could not modify the inert conditions near the powders. This explanation is consistent with complementary DSC experiments carried out on powders and one film. In Fig. 2b, we realize that, when treated in the same conditions (100 mL/min of Ar), the film reacts with oxygen giving rise to a highly exothermic peak, whereas the decomposition of powders is endothermic as if the atmosphere was completely inert. In other words, we can conclude that films are much more sensitive than powders to traces of oxygen or any reactive gas during pyrolysis.

III.2.- Evolution of gaseous species: decomposition of $Ba(TFA)_2$

Local atmosphere composition near the sample can also be affected by the volatiles that result from decomposition and, due to the reverse reaction, a higher concentration of products may reduce the overall reaction rate. This effect is very common in carbonates, whose decomposition temperature is lowered by hundreds of degrees when the sample mass is reduced, due to the lower local concentration of CO_2. It has also been reported in the studies devoted to determine the decomposition temperature of YBCO at very low oxygen partial pressures [21]. The reduction of T_{dec} in $Ba(TFA)_2$ films with respect to powders (Fig. 3) can be explained in a similar way.

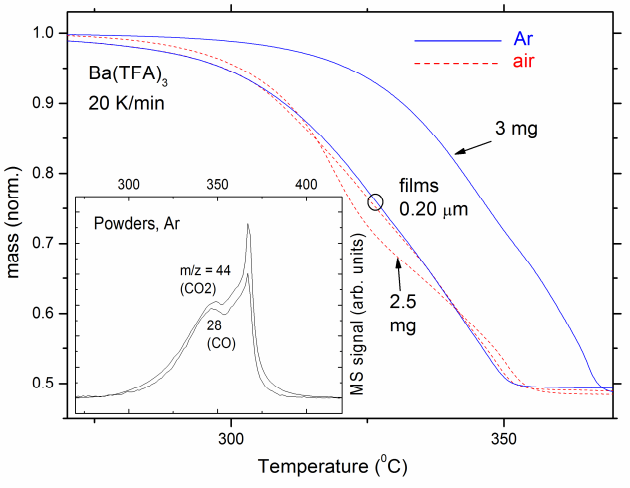

Figure 3.- TG curves of $Ba(TFA)_2$ powders and films decomposition in Ar and air. Inset: MS curves of CO and CO_2 measured during powder decomposition in Ar.

First of all, notice that $Ba(TFA)_2$ powders decompose at a lower temperature in air than in Ar (Fig. 3). Although this fact may induce to think that decomposition is triggered by reaction with oxygen, this is not the case. DSC measurements show that the decomposition enthalpy is more exothermic in air by just the heat evolved during the oxidation of one mol of CO to CO_2 [22]. In other words, oxygen molecules do not participate in the primary decomposition reaction but in a secondary reaction with CO out of the sample. This fact, together with MS results, notably the equal amounts of CO and CO_2 detected in inert atmosphere (inset of Fig. 3), led us to propose the following overall decomposition reaction:

$$Ba(TFA)_2 \text{ -----> } BaF_2 + CF_3CFO + CO_2 + CO. \qquad (1)$$

So, in air oxygen reacts with CO and reduces its concentration near the sample, thus reducing the inverse reaction rate and enhancing the decomposition rate in powders (i.e., lowering T_{dec}).

On the contrary, experiments carried out in films show that their T_{dec} is identical in air than in Ar [23] and lower than for powders in Ar (Fig. 3). This result is coherent with reaction (1) if gas exchange is so easy in films that CO concentration is so low that the reverse reaction can be neglected even in the absence of oxygen.

This example tells us that, even if T_{dec} clearly depends on the presence of reactive gas species (usually O_2) in powders, this dependence may be lost when dealing with films.

III.3.- Heat transport: combustion of Cu acetate

When decomposition of metal organic compounds takes place in air or in pure oxygen, the process is highly exothermic. Consequently, the sample temperature will be higher than that measured by the TG apparatus and indicated on the x-axis of a mass-loss curve. This sample overheating will depend on the heat dissipation paths. For large samples in powder form, the process will be more adiabatic and, eventually, combustion can occur. Combustion begins with a local overheating that leads to local thermal runaway (ignition) that propagates all along the sample as a combustion front. This phenomenon can be identified in a TG curve by an abrupt mass loss (solid curve in Fig. 4) that often begins with a slope discontinuity. Decomposition reaches completion in few seconds indicating that the local temperature at the combustion front is hundreds of Celsius above the measured temperature [24].

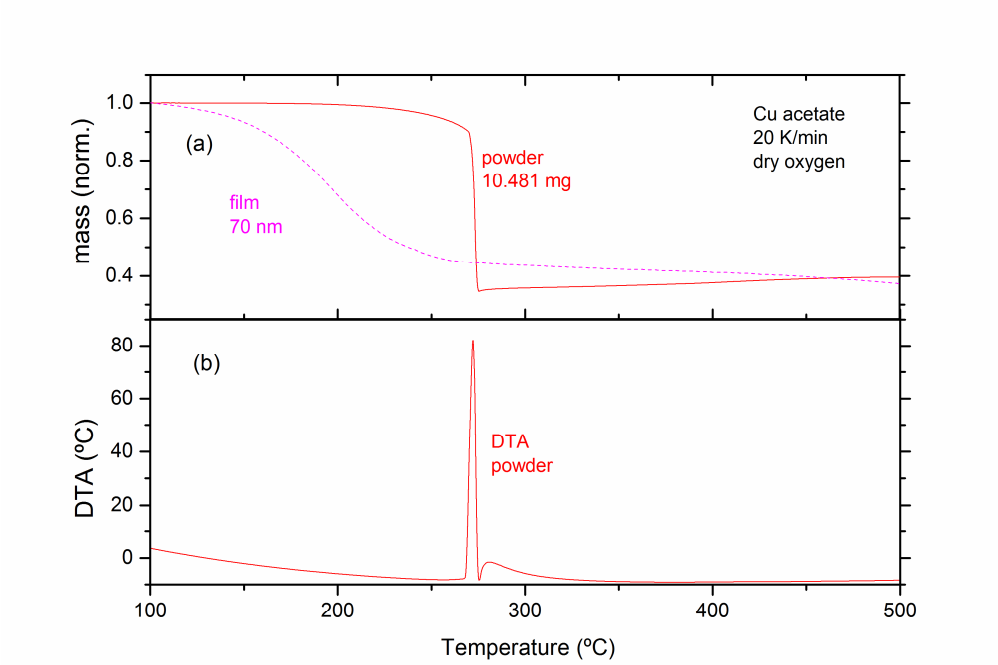

Figure 4.- a) TG decomposition curves of Cu acetate in dry oxygen for powders and one film; b) the corresponding DTA curve for the powder showing that its decomposition entails high overheating of the sample leading to combustion (*the DTA signal from the film was below the apparatus sensitivity)*.

Combustion synthesis has been recently proposed as a general route for the low-temperature fabrication of oxide thin films [7]. However, calculations shown that the very high thermal conductance between the substrate and the film makes it very difficult to reach the overheating needed for combustion and, consequently, we think that combustion of thin films (say, below 1 μm) is very unlikely [25]. In fact, we have observed combustion in several precursor powders but this phenomenon was always absent for the corresponding films. The case of Cu acetate in dry oxygen constitutes a nice example (Fig. 4).

Due to the oxygen depletion effect discussed above, decomposition of Cu acetate powders begins at a temperature higher than that of films. For the experiment reported in Fig. 4, decomposition of powders becomes unstable at 270ºC where the abrupt mass loss indicates that combustion occurs. This mass-loss event is accompanied by a sharp differential thermal analysis (DTA) peak indicating a sudden heat evolution (Fig. 4b). Although, the DTA gauge recorded a sample overheating of 80ºC, the local temperature at the combustion front is much higher. The interesting point here is that, in contrast with powders, the film TG curve is smooth (dotted curve in Fig. 4a), i.e. no combustion takes place.

The first three examples discussed so far (Ce propionate, $Ba(TFA)_2$ and Cu acetate) lead us to point out that, in general, films decompose at a temperature lower than powders. Therefore, researchers interested in low-temperature processing of CSD films should take it into account. We have recently shown that ceria films can be obtained at a temperature as low as 160ºC from Ce propionate [12]. Similarly, CuO nanocrystalline films can be obtained at 180ºC through isothermal decomposition of Cu acetate. The XRD curves of powders and a thin film treated at 180 ºC for 1 h are shown in Fig. 5. Whereas Cu acetate remains the dominant phase (perhaps the only phase) in the powders, the film has been decomposed into CuO.

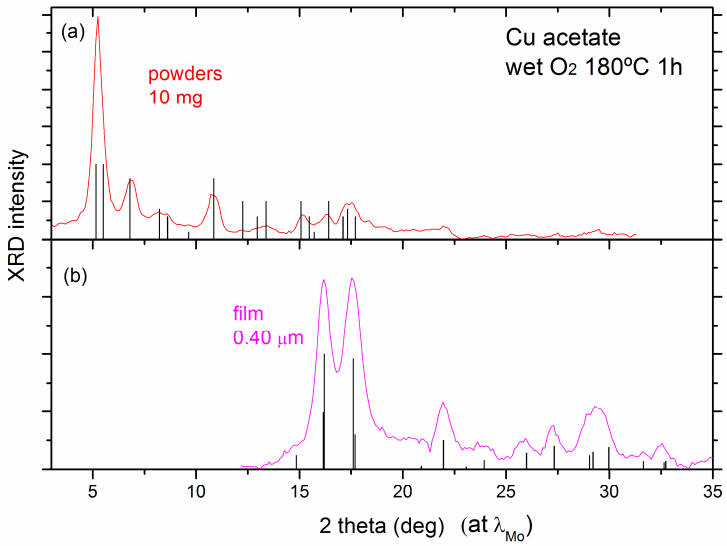

Figure 5.- XRD of the product of Cu acetate after heat treatment at 180ºC lasting 1 h in wet O_2. The curve of powders (a) has the characteristic peaks of Cu acetate (i.e. no decomposition has occurred), whereas, the curve of one film (b) corresponds to CuO.

The two last examples that follow deal with the differences between films and powders with respect to the formation and stability of intermediate decomposition products.

III.4.- Gas exchange and combustion: reduction of Cu

In some cases, decomposition of metal organic precursors entails a change in the metal oxidation state. Decomposition of Au [26], Ni [27] and Ag acetates [28] in an inert atmosphere leads to the formation of metallic nanoparticles, whereas oxidation of Ce(III) into Ce(IV) is usually observed for ceria precursors even in an inert atmosphere [20]. The effect of oxidizing or reducing species produced during decomposition or coming from the furnace atmosphere will depend, in general, on their transport across

the sample. Since this transport is easier in films than in powders, differences of the oxidation state may be expected between films and powders. This point will be analyzed for the particular case of Cu acetate decomposition in dry oxygen.

Let us analyze first the TG curves measured on varying amounts of powder that are plotted together in Fig. 6. To deduce the nature of the decomposition products, the masses of CuO, Cu_2O and metallic Cu are indicated as horizontal lines. Note that at 600ºC where the mass becomes stable (no further increment is observed above this temperature), all the curves lay below the mass of CuO (the only thermodynamically stable state in dry oxygen at this temperature). This means that some Cu has been lost during decomposition due to precursor evaporation. This effect is well known in YBCO thin film growth processes by CSD, where an initial excess of Cu precursor to compensate for it is used or decomposition is done in a wet atmosphere to avoid the evaporation of the Cu precursor [29] and has also been reported for other metal oxide precursors [30]. Anyway, the feature we are interested in is the smooth mass gain observed in powders after decomposition. It corresponds to the oxidation of Cu_2O or metallic Cu into CuO [31]. This process indicates that, despite the highly oxidative furnace conditions, copper becomes partially (or highly) reduced during decomposition. Recently, *in situ* XRD measurements during heating ramps have shown the successive states of oxidation that Cu acquires during decomposition on Cu acetate powders [32].

The degree of Cu reduction during decomposition can be estimated by the mass-gain that is observed after decomposition, because Cu and Cu_2O will become fully oxidized when the temperature is raised in an oxidative atmosphere. So, the mass gain measured from the end of decomposition up to 600ºC, (see the definition of in Fig. 6), is just a measure of the degree of reduction that copper has experienced during decomposition. From the TG curves of Fig. 6, it is clear that Cu reduction is lower for smaller m_i. This result is, as expected, according to the general argument that the out-diffusion of reducing species formed during decomposition [31] and the transport of oxygen into the sample is easier for smaller amounts of powder. In addition, combustion also contributes to this result. Since the decomposition rate is very high at the combustion front, the concentration of reducing volatile species there will be also very high and will partially displace oxygen, making the local atmosphere more reducing than in the absence of combustion. Since combustion (i.e. the abrupt step on the TG curves) accounts for almost the 100% of the mass-loss for the largest sample whereas it accounts roughly for

50% of the mass-loss for the smallest sample, we deduce that copper reduction during decomposition must be more pronounced as m_i increases, as observed.

In the absence of combustion, thin films should experience minimum Cu reduction. Unfortunately, the Cu reduction feature characteristic of the TG curves of powders is absent from the curve of a thin film because decomposition still continues up to around 500 ºC (Fig. 6) making it impossible to extract its degree of reduction. We can try to estimate it in thin films by extrapolating the results of powders to $m_i = 0$. From the inset of Fig. 6, it is clear that the degree of copper reduction will be very small in films. We have verified it by XRD measurements on powders and a film treated up to 300ºC (Fig. 7). The diffraction curve obtained on 10 mg of powders indicates that CuO is the residual phase whereas it is the only phase detected in the film (i.e. no Cu reduction is observed after decomposition of Cu acetate films in dry oxygen).

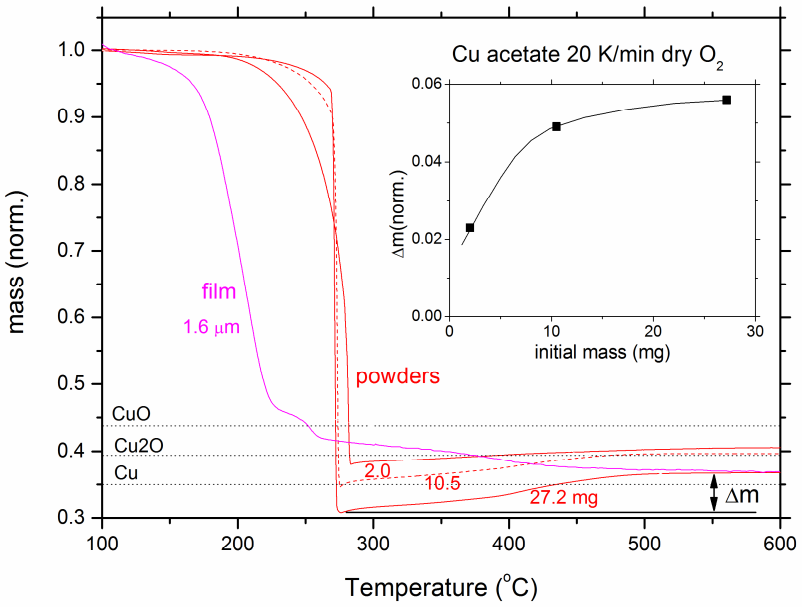

Figure 6.- Comparison between the TG decomposition curves of Cu acetate powders and one film in dry oxygen. The y-axis of the inset corresponds to the mass increment due to complete oxidation of Cu and Cu_2O (see arrow in the main figure). The solid curve shows the general trend.

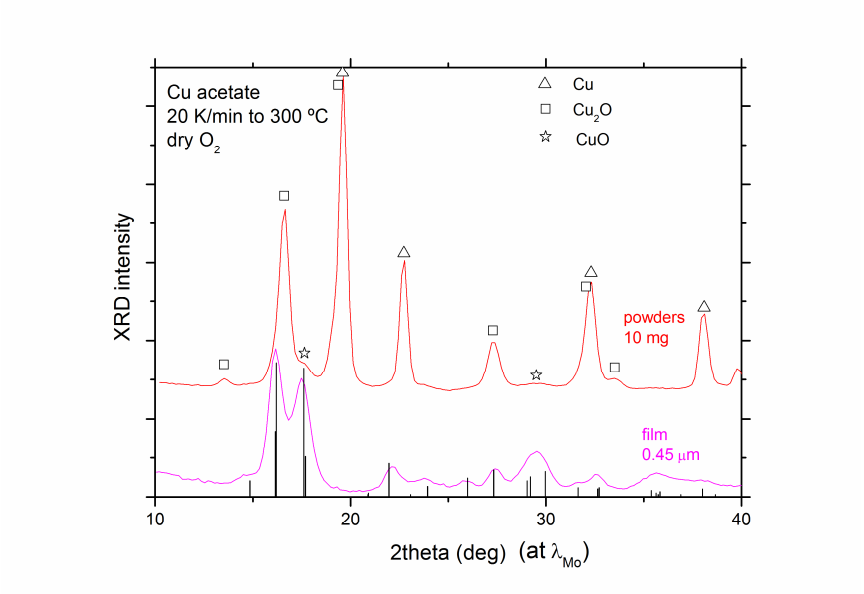

Figure 7.- XRD curves of Cu acetate treated up to 300ºC in dry oxygen (vertical bars: expected peaks for CuO). Whereas copper is highly reduced in the powder, it is fully oxidized in the film.

This example illustrates that, when used uncritically, the results on powders can lead to very erroneous conclusions for films (e.g. from any individual TG curve one would deduce a high reduction degree). However, when treated with caution, from the trend of the powders at the limit of zero initial mass we can deduce the approximate behaviour of films.

III.5.- Stability of intermediate products: metal fluorides and YBCO formation

Although the usual aim of CSD is to obtain oxide films, sometimes decomposition of the precursor molecule leads to the formation of intermediate products such as metal carbonates or fluorides [2, 16, 19]. In fact, at present, the most promising precursors for YBCO production are fluorine-based [4, 19]. With this choice, maximum critical currents are obtained. However, if we trusted on the thermal analysis of powders, we should conclude that this solution would be far from satisfactory because of the abundance of BaF_2 in their decomposition product.

$Y(TFA)_3$ powders decompose into fluorides and oxyfluorides that are stable up to 1000ºC (Fig.8a), a temperature much higher than that of YBCO film formation (around 800ºC). The product of $Ba(TFA)_2$ decomposition (BaF_2) is still much more stable. One can see in Fig. 8b that BaF_2 begins to decompose above 1200ºC. Furthermore, we have treated a powder mixture obtained by precipitation from a solution containing the Y and Ba TFA precursors with molar ratio Y:Ba = 1:2, because studies on the mechanism of YBCO formation [19] indicate that Y and Ba fluorides are less stable when obtained

from the mixture. The corresponding TG curve of Fig. 8c shows a mass loss step at 750ºC. The final mass at 810ºC has a value coherent with a mixture of BaF_2, YOF and Y_2O_3. In fact, XRD measurements reveal that the product contains two Ba oxyfluoride phases plus BaF_2 and a complex fluoride of Ba and Y (Fig. 9), i.e., no oxides have been produced at the temperature that is used to obtain YBCO films. Consequently, thermal analysis of powders would lead to the erroneous prediction that YBCO preparation is not possible from TFA precursors.

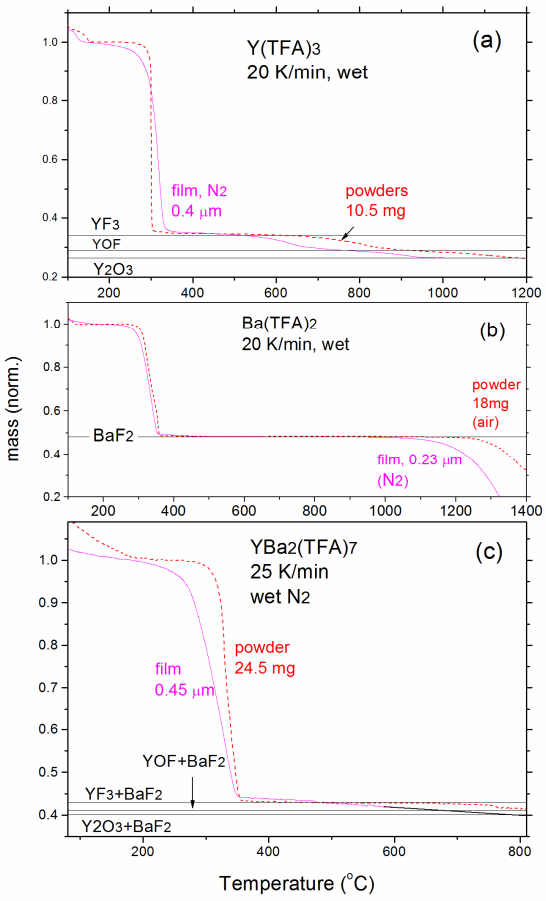

Figure 8.- TG curves of the decomposition of powders and films of Y(TFA)3 (a), Ba(TFA)2 (b) and a binary TFA precursor with molar ratio Ba:Y = 2:1 (c).

If we repeat these experiments with films, the result is quite different. Both BaF_2 and YF_3 films are less stable than powders; their decomposition temperature is lower by more than 100ºC (Figs. 8a and 8b). The stability of Y fluoride is still lower if films are obtained from the binary solution. Just after precursor decomposition, above 400ºC, their corresponding TG curve (Fig. 8c) has a negative slope, and the mass at 800ºC suggests that no Y fluoride phases exist at this temperature. This point is nicely

confirmed by the XRD curve measured on this film, where Y_2O_3 is the only phase containing Y, all the Y fluorinated phases have disappeared and the main Ba-related phase is BaF_2 (Fig. 9).

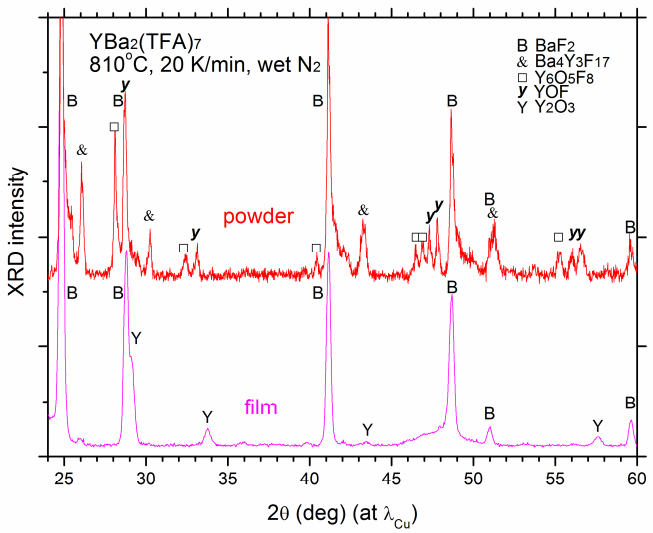

Figure 9.- XRD of the products of decomposition of a binary $Y(TFA)_3/2Ba(TFA)_2$ precursor in wet nitrogen after heating them up to 810ºC in wet N_2.

The different behaviour of films can be explained by the fact that, thanks to the enhanced gas transport of volatiles or reactive gases, intermediate products tend to be less stable in films than in powders. In the particular case of metal fluorides, it has been shown that they decompose by reaction with water vapour and that the rate-limiting step is HF out-diffusion [14, 33]. Therefore, its faster diffusion in films explains their lower decomposition temperature.

Despite the improved behaviour of films and, in particular, of the binary film, BaF_2 still survives at 800ºC, thus precluding YBCO formation. Since YBCO films are prepared at this temperature, we must conclude that BaF_2 stability is lower when $Cu(TFA)_2$ precursor enters into play. To reveal this effect, a ternary solution of Y, Ba and Cu TFA precursors with molar ratio 1:2:3 has been prepared and, after precipitation, it has been heat treated in wet nitrogen. The complexity of this particular precursor mixture makes it very difficult to reach any conclusion about the nature of the products from the TG curves. So, we have analysed them by XRD.

One film of the ternary precursor with 0.9 µm of nominal thickness was deposited on silicon substrates protected by a nanometric Y_2O_3 film and after treating it at 810ºC during 30 min, its product has been compared with that of 9 mg of powders treated at 920ºC. We have taken silicon instead of the

substrates used for YBCO film production to avoid epitaxial crystallization, so that the observed differences between the film and powders can be unambiguously related to gas transport.

The XRD curve of powders (Fig.10a) shows that BaF_2 is still the only Ba-containing crystalline phase like in the binary precursor; i.e., apparently, copper atoms have not diminished the stability of this phase. On the contrary, one can notice (Fig. 10b) an important diminution of the BaF_2 content in the film. This result on the film is coherent with the interpretation that gas transport makes it easier YBCO synthesis in thin films than in powders even if epitaxial crystallization is prevented by using a silicon substrate.

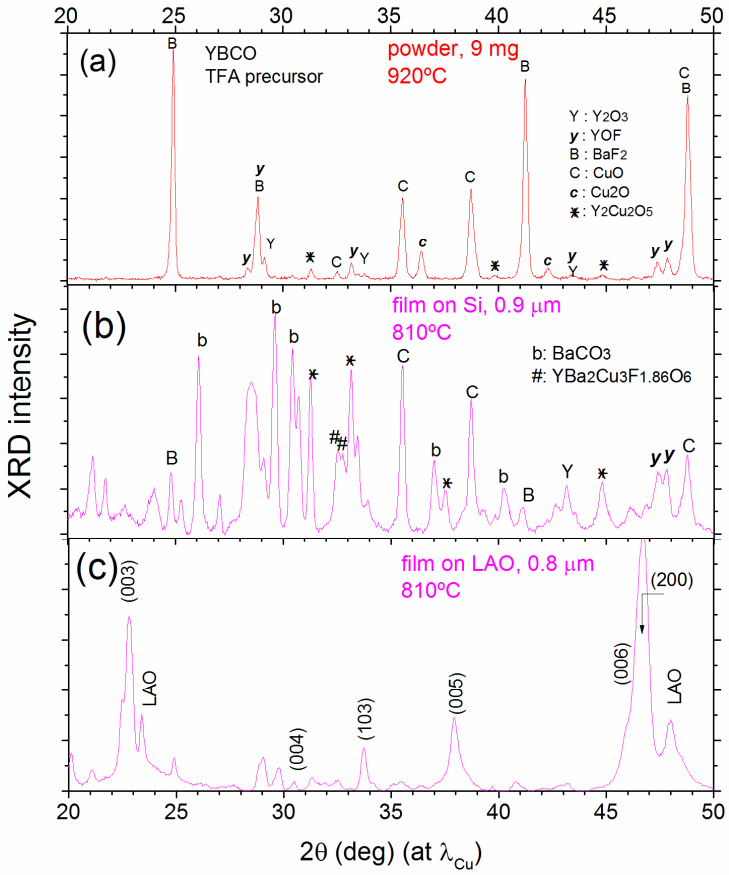

Figure 10.- XRD of the decomposition products of a ternary 1:2:3 Y:Ba:Cu TFA precursor in the form of powders (a), in a film deposited on silicon (b) and on (001)$LaAlO_3$ (LAO) single crystalline substrate (c). The indexed peaks in (c) refer to YBCO.

Before leaving this section, we should remark that films on $LaAlO_3$ substrates (where epitaxial crystallization occurs) treated at identical conditions are completely transformed into YBCO (Fig. 10c). This means that lattice match with the substrate does not only make possible epitaxy but it activates the reaction between the component oxides of YBCO.

IV.- Conclusions

The examples given above clearly show that films of metal organic precursors decompose differently than their corresponding powders: a) their decomposition temperature is lower; b) decomposition via combustion does not occur (so far, we have not found a single exception to these two conclusions); c) films are more sensitive to residual amounts of oxygen in the furnace atmosphere and d) the intermediate products obtained before oxide formation are less stable. These differences arise because of the larger surface to volume ratio of films that facilitate gas and heat exchange and raise the question about the usefulness of doing thermal analyses on powders for predicting the behaviour of films.

After decades of doing thermal analysis on powders by people that make films, any intention of discrediting this practice is nonsense. We want simply to remark that not only quantitative information may not be accurate enough (e.g. the decomposition temperature) but that even qualitative conclusions may be erroneous (e.g. combustion of films). In those cases where the decomposition evolves with the mass of powders, this evolution can serve to predict the behaviour of films. However, in the absence of such an evolution, the behaviour of films can only be deduced by general rules like those indicated in the previous paragraph.

We thus conclude that thermal analysis on films is very useful for the analysis of the preparation of oxide films and may be unavoidable in some instances. Although the sample mass must be lower than with powders, films of 1 mg may already deliver significant results. This amount of sample can be analyzed without much difficulty by modern TG/DTA and DSC equipment.

Acknowledgments

We acknowledge the financial support from MICINN (MAT2011-28874-C02-01 and -02, Consolider Project NANOSELECT: CSD2007-00041), EU project EUROTAPES, (EUFP7 NMPLA2012280432) and by the Generalitat de Catalunya (Pla de Recerca 2009SGR-185, 2009-SGR-770 and XaRMAE). H.Eloussifi acknowledges financial support from the Tunisian Ministry of Higher Education and Scientific Research. The authors are indebted to Dr.Joan Pere López Olmedo and Dr.Xavier Fontrodona of STR, University of Girona, and Dr.Josep Bassas of CCT, University of Barcelona, for their technical assistance.

References.-

[1] Lange, F.F. Chemical Solution Routes to Single-Crystal Thin Films, *Science* **1996**, *273***,** 903-909.

[2] Schwartz, R.; Schneller, T.; Waser, R. Chemical Solution Deposition of Electronic Oxide Films, *C. R. Chimie* **2004**, *7*, 433-461.

[3] Bhuiyan, M.S.; Paranthaman, M.; Salama, K. Solution-Derived Textured Oxide Thin Films - A Review, *Supercond.Sci.Technol.* **2006**, *19*, R1-R21.

[4] Obradors, X.; Puig, T.; Pomar, A.; Sandiumenge, F.; Mestres, N.; Coll, M.; Cavallaro, A.; Roma, N.; Gazquez, J.; Gonzalez, J.C.; et al., Progress Towards All-Chemical Superconducting $YBa_2Cu_3O_7$-Coated Conductors, *Supercond. Sci. Technol*. **2006**, *19*, S13-S26.

[5] Gibert, M.; Puig, T.; Obradors, X.; Benedetti, A.; Sandiumenge, F.; Huhne, R. Self-Organization of Heteroepitaxial CeO_2 Nanodots Grown from Chemical Solutions, *Adv. Mater.*, **2007**, *19*, 3937-3942.

[6] Cavallaro, A.; Sandiumenge, F.; Gazquez, J.; Puig, T.; Obradors, X.; Arbiol, J.; Freyhardt, H.C. Growth Mechanism, Microstructure, and Surface Modification of Nanostructured CeO_2 Films by Chemical Solution Deposition, *Adv. Funct. Mater*. **2006**, *16*, 1363-1372.

[7] Kim, M.-G.; Kanatzidis, M.G.; Facchetti, A.; Marks, T.J. Low-Temperature Fabrication of High-Performance Metal Oxide Thin-Film Electronics Via Combustion Processing, *Nature Materials* **2011**, *10*, 382-388.

[8] Schoop, U.; Rupich, M.W.; Thieme, C.; Verebelyi, D.T.; Zhang, W.; Li, X.; Kodenkandath, T.; Nguyen, N.; Siegal, E.; Civale, L. et al., Second Generation HTS Wire Based on Rabits Substrates and MOD YBCO, *IEEE Trans. Appl. Supercond*. **2005**, *15*, 2611-2616.

[9] Rupich, M.W.; Li, X.P.; Thieme, C.; Sathyamurthy, S.; Fleshler, S.; Tucker, D.; Thompson, E.; Schreiber, J.; Lynch, J.; Buczek, D.; et al., Advances In Second Generation High Temperature Superconducting Wire Manufacturing And R&D at American Superconductor Corporation, *Supercond. Sci. Technol*. **2010,** *23*, 014015.

[10] Obradors, X.; Puig, T. Coated Conductors for Power Applications: Materials Challenges, *Supercond. Sci. Technol* **2014**, *27*, 044003.

[11] Todorov, T.; Cordoncillo, E.; Sanchez-Royo, J.F.; Carda, J.; Escribano, P. $CuInS_2$ Films for Photovoltaic Applications Deposited by a Low-Cost Method, *Chem.Mater*. **2006,** *18*, 3145-3150.

[12] Roura, P.; Farjas, J.; Ricart, S.; Aklalouch, M.; Guzman, R. et al. Synthesis of Nanocrystalline Ceria Thin Films by Low-Temperature Thermal Decomposition of Ce-Propionate, *Thin Solid Films* **2012,** *520*, 1949-1953**.**

[13] Bassiri-Gharb, N.; Bastani, Y.; Bernal, A. Chemical Solution Growth of Ferroelectric Oxide Thin Films and Nanostructures, *Chem. Soc. Rev.*, **2014**, *43*, 2125-2140.

[14] Eloussifi, H. ; Farjas, J. ; Roura, P. ; Dammak, M. Evolution of Yttrium Trifluoroacetate During Thermal Decomposition, *J.Term.Anal.Calorim.* **2012**, *108*, 597-603.

[15] Jeong, S.; Lee, J-Y.; Lee, S.S.; Choi, Y.; Ryu, B.H. Impact of Metal Salt Precursor on Low-Temperature Annealed Solution-Derived Ga-doped In2O3 Semiconductor for Thin-Film Transistors, *J.Phys.Chem.C* **2011**, *115*, 11773-11780.

[16] Llordes, A.; Zalamova, K.; Ricart, S.; Palau, A.; Pomar, A.; Puig, T.; Hardy, A.; van Bael, M.K.; Obradors, X., Evolution of Metal-Trifluoroacetate Precursors in the Thermal Decomposition toward High-Performance YBa2Cu3O7 Superconducting Films, *Chem.Mater*. **2010**, *22*, 1686-1964.

[17] Farjas, J.; Pinyol, A.; Rath, Ch.; Roura, P.; Bertran, E. Kinetic Study of the Oxide-Assisted Catalyst-Free Synthesis of Silicon Nitride Nanowires, *Phys. Stat. Sol. A* **2006**, *203*, 1307-1312.

[18] Eloussifi, H.; Farjas, J.; Roura, P.; Ricart, S.; Puig, T.; Obradors, X.; Dammak, M. Thermoanalytical Study of the Decomposition of Yttrium Trifluoroacetate Thin Films, *Thin Solid Films* **2013**, *545*, 200-204.

[19] Obradors, X.; Puig, T.; Ricart, S.; Coll, M.; Gazquez, J.; Palau, A.; Granados, X. Growth, Nanostructure and Vortex Pinning in Superconducting $YBa_2Cu_3O_7$ Thin Films based on Trifluoroacetate Solutions, *Supercond. Sci.Tecnol.* **2012**, *25*, 12301.

[20] Roura, P.; Farjas, J.; Camps, J.; Ricart, S.; Arbiol, J.; Puig, T.; Obradors, X. Decomposition Processes and Structural Transformations of Cerium Propionate into Nanocrystalline Ceria at Different Oxygen Partial Pressures, *J. Nanopart. Res.* **2011**, *13*, 4085-4096.

[21] Lindemer, T.B.; Washburn, F.A.; MacDougall, C.S.; Feenstra, R.; Cavin, O.B. Decomposition of $YBa_2Cu_3O_7$-X and $YBa_2Cu_4O_8$ for PO_2 < 0.1 MPa, *Physica C*, **1991**, *178*, 93-104.

[22] Farjas, J.; Camps, J.; Roura, P.; Ricart, S.; Puig, T.; Obradors, X. The Thermal Decomposition of Barium Trifluoroacetate, *Thermochim.Acta*, **2012**, *544*, 77-83.

[23] Eloussifi, H.; Farjas, J.; Roura, P.; Ricart, S.; Puig, T.; Obradors, X.; Dammak, M. Thermal Decomposition of Barium Trifluoroacetate Thin Films, *Termochim.Acta*, **2013**, *556***,** 58-62.

[24] Chen, W.; Li, F.; Yu, J. Combustion Synthesis and Characterization of Nanocrystalline CeO2-based Powders Via Ethylene Glycol-Nitrate Process *Mater.Lett.* **2006**, *60*, 57-62.

[25] Sanchez-Rodriquez, D.; Farjas, J.; Roura, P.; Ricart, S.; Mestres, N.; Obradors, X.; Puig, T. Thermal Analysis for Low Temperature Synthesis of Oxide Thin Films from Chemical Solutions, *J.Phys.Chem.C* **2013**, *117*, 20133-20138.

[26] Bakrania, S.D.; Rathore, G.K.; Wooldridge, S. An Investigation of The Thermal Decomposition of Gold Acetate *J. Therm. Anal. Cal.* **2009**, *95*, 117-122.

[27] De Jesus, J.C.; Gonzalez, I.; Quevedo, A.; Puerta, T. Thermal Decomposition of Nickel Acetate Tetrahydrate: an Integrated Study by TGA, QMS and XPS Techniques *J. Molec. Catal. A: Chem*. **2005**, *228*, 283-291.

[28] Logvinenko, V.; Polunina, O.; Mikhailov, K.; Bokhonov, B. Study of Thermal Decomposition of Silver Acetate, *J. Therm. Anal. Cal.* **2007**, *90*, 813-816.

[29] Dawley, J.T.; Clem, P.G.; Boyle, T.J.; Ottley, L.M.; Overmyer, D.L.; Siegal, M.P. Rapid Processing Method for Solution Deposited $YBa_2Cu_3O_{7-\delta}$ Thin Films *Physica C-Superconductivity and Its Applications* **2004**, *402*, 43-151.

[30] Arii, T.; Kishi, A. The Effect of Humidity on Thermal Process of Zinc Acetate, *Thermochim.Acta*. **2003**, *400*, 175-185.

[31] Lin, Z.; Han, D.; Li, S. Study on Thermal Decomposition of Copper(II) Acetate Monohydrate in Air, *J. Therm. Anal. Cal.* **2012**, *107*, 471-475.

[32] Kondrat, S.A.; Davies, T.E.; Zu, Z.; Boldrin, P.; Bartley, J.K.; Carley, A.F.; Taylor, S.H.; Rosseinsky, M.J.; Hutchings, G.J. The Effect of Heat Treatment on Phase Formation of Copper Manganese Oxide: Influence on Catalytic Activity for Ambient Temperature Carbon Monoxide Oxidation, *J. Catal.* **2011**, *281*, 279-289.

[33] Eloussifi, H.; Farjas, J.; Roura, P.; Camps, J.; Dammak, M.; Ricart, S.; Puig, T.; Obradors, X. Evolution of Yttrium Trifluoroacetate during Thermal Decomposition, *J.Therm. Anal. Calorim.* **2012**, *108*, 589-596.

for TOC only

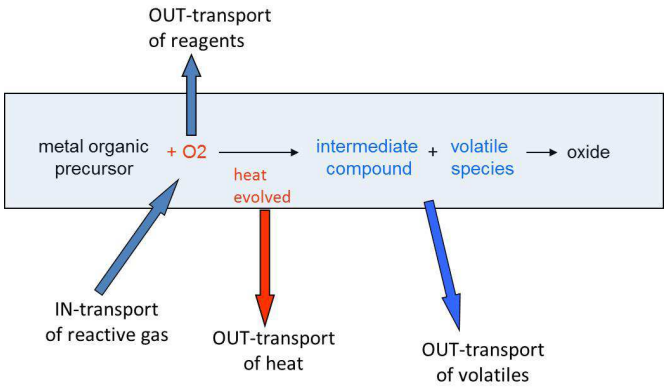
OUT-transport
of reagents
metal organic
precursor
+ O2
heat
evolved
intermediate
compound
+
volatile
species
oxide
IN-transport
of reactive gas
OUT-transport
of heat
OUT-transport
of volatiles